PCCP

Accepted Manuscript

ROYAL SOCIETY OF CHEMISTRY

www.rsc.org/pccp

PCCP RSCPublishing

ARTICLE

Cite this: DOI: 10.1039/x0xx00000x

Received 00th January 2012,
Accepted 00th January 2012

DOI: 10.1039/x0xx00000x

www.rsc.org/

Efficient Intersystem Crossing Using Singly Halogenated Carbomethoxyphenyl Porphyrins Measured Using Delayed Fluorescence, Chemical Quenching, and Singlet Oxygen Emission

Dawn M. Marin, Sonia Payerpaj, Graham S. Collier, Angy L. Ortiz, Gaurav Singh, Marcus Jones, Michael G. Walter*

ABSTRACT: Sensitizers with high triplet quantum yields are useful for generating photovoltaics, photocatalysts and photodynamic therapy agents with increased efficiency. In this study, the heavy atom effect was used to optimize the triplet and singlet oxygen quantum yields of 5,10,15,20-tetrakis(4-carbomethoxyphenyl)porphyrin (1-TCM_4PP). The triplet quantum yields, determined using delayed fluorescence, was calculated as 0.35 for 1-TCM_4PP, 0.75 for 5,10,15-tris(4-carbomethoxyphenyl)-20-(4-bromophenyl)porphyrin (2-$TBCM_3PP$) and 0.88 for 5,10,15-tris(4-carbomethoxyphenyl)-20-(4-iodophenyl)porphyrin (3-TCM_3IPP). Chemical quenching of 1,3-diphenyisobenzofuran and singlet oxygen emission studies rendered an average singlet oxygen quantum yield of 0.51, 0.75, and 0.90 for TCM_4PP, $TBCM_3PP$ and TCM_3IPP respectively. These photophysical properties indicate that a single halogen atom is capable of transforming TCM_4PP into a sensitizer with strong triplet character. This is useful for generating singlet oxygen for photodynamic therapy, creating a long lasting reactive species for catalysis and for extending diffusion lengths in photovoltaic applications while retaining three molecular modification points for further functionalization.

Introduction

Porphyrins are organic semiconducting molecules extensively researched for use in solar energy conversion, light induced chemical catalysis, imaging and therapeutics.[1, 2] Their incorporation into these diverse technologies can be attributed to their unique photo-physical properties that can be modified through chemical engineering and device architecture. Once an exciton is generated via light absorption, the electron populates the excited singlet state. One distinguishing feature of porphyrins is their ability to undergo intersystem crossing, normally a spin forbidden process, from the singlet into the triplet excited state. Porphyrin sensitizers with high efficiencies of triplet formation can be used to improve the efficiency of photovoltaics and photo-catalysts because the triplet state has a characteristically long lifetime.[3] This allows excitons more time to diffuse to an interface before recombining and provides a longer lasting reactive species for catalysis.[4, 5] The triplet state of a porphyrin is also capable of creating singlet oxygen, a powerful oxidant that can damage tumor cells for therapeutic purposes.[1, 2]

One approach to increase the efficiency of triplet formation is to covalently attach or coordinate a heavy atom, such as a halogen or transition metal, to the porphyrin structure.[6-9] Heavy atoms promote intersystem crossing into the triplet state due to spin orbit coupling.[10] Studies have demonstrated that a single bromine or iodine substituent at the β pyrrole or meso position of octaethylporphyrin increases the triplet quantum yield up to 85%.[6] However a bromine atom in the meso position can cause buckling of the porphyrin core and halogen atoms on the β pyrrole position increases the rate of triplet decay.[6, 7] Similar molecules with multiple halogen atoms located on the phenyl rings of tetraphenylporphyrin derivatives show that the triplet quantum yield generally increases with an increase in the size of the heavy atom.[6-9, 11-13] However information gleaned from these studies is complicated due to the number, variety and different positions of heavy atom substituents as well as the different parameters reported for each study. The significance of the following research is that it demonstrates the effect of a single halogen atom substitution for one carbomethoxy substituent on one of the phenyl rings of 5,10,15,20-tetrakis(4-carbomethoxyphenyl)porphyrin. The use of only a single halogen is advantageous because it allows the remaining three carbomethoxy groups on the meso phenyl rings of the porphyrin core to act as molecular modification points for further functionalization. The structures of the different carbomethoxyphenylporphyrin derivatives studied are shown in Fig 1.

In order to successfully engineer these newly synthesized porphyrin dyes into solar cells or use them as photo-catalysts or photodynamic therapy agents, the photophysical properties of the dyes in solution were determined. The photophysical properties include 1) absorption and emission profiles, 2) rates of conversion, 3) lifetimes and 4) the efficiency with which the singlet and triplet excited states form. The work presented here complements Weisman's triplet-triplet annihilation method to determine triplet quantum yields.[14] Both the delayed fluorescence and the fast singlet fluorescence can be measured using the same time resolved fluorescence setup with a gated multi-pulsed excitation technique.[15] In addition, a comparison of the singlet oxygen quantum yields obtained using two different techniques is presented.

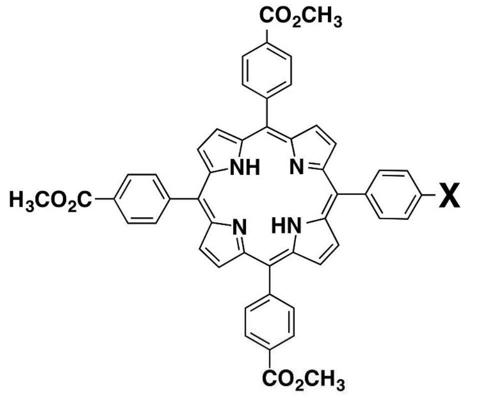

1: X = CO_2CH_3 - 5,10,15,20-tetrakis(4-carbomethoxyphenyl)porphyrin
2: X = Br - 5,10,15,-tris(4-carbomethoxyphenyl)-20-(4-bromophenyl)porphyrin
3: X = I - 5,10,15-tris(4-carbomethoxyphenyl)-20-(4-iodophenyl)porphyrin

Fig 1. The structures and names of the three different carbomethoxyphenylporphyrin derivatives characterized in this study. The following abbreviations are used: 1 = TCM_4PP, 2 = $TBCM_3PP$ and 3 = TCM_3IPP.

Results and Discussion

Absorption and Emission Spectra

The absorption and emission spectra for (1) TCM_4PP, (2) $TBCM_3PP$ and (3) TCM_3IPP are shown in Fig. 2 and Fig. 3. All three derivatives have identical molar absorptivities and absorption peaks in the Soret band region (350 nm – 450 nm) and four Q bands (500 nm - 650 nm).[16] The emission spectra show peaks at approximately 653 nm and 717 nm. (1) TCM_4PP exhibits the highest fluorescence, followed by (2) $TBCM_3PP$ and (3) TCM_3IPP.

Lifetimes and Singlet Excited State Quantum Yields

The fluorescence lifetime decay profiles for the porphyrin derivatives are depicted in Fig. 4. The fluorescence lifetimes (τ_F), fluorescence quantum yields (ϕ_F), and fluorescence radiative decay rates (k_F) are listed in Table 1. Both Fig. 4 and Table 1 show that (1) TCM_4PP has the longest lifetime of 9.22 ns, followed by (2) $TBCM_3PP$ with a lifetime of 5.26 ns and then (3) TCM_3IPP with the shortest lifetime of 2.22 ns. Fluorescence quantum yields for TCM_4PP, $TBCM_3PP$ and TCM_3IPP were calculated using the comparative method, as shown in equation 1.[17-20] Tetratolylporphyrin was used as the reference, with a quantum yield of 0.11 in DCM.[17, 18, 21]

$$\phi = \phi_{Std} \frac{m}{m_{Std}} \frac{n^2}{n_{Std}^2} \qquad (1)$$

In equation 1, ϕ represents the fluorescence quantum yield, m represents the slope when the area of the emission peak is plotted against the absorption of the fluorophore at the excitation wavelength at various concentrations. The subscript *Std* represents the variables for the reference compound and n is the refractive index of the solvent. The fluorescent quantum yields also decreased with halogenation and were determined to be 0.09, 0.04 and 0.02 for (1) TCM_4PP, (2) $TBCM_3PP$ and (3) TCM_3IPP respectively. The fluorescence quantum yield and lifetime obtained for TCM_4PP in DCM are similar to those reported in chloroform with a ϕ_F of 0.11 and a τ_F of 9.2 ns.[12] The decreasing trend in the fluorescence emission, lifetime and quantum yield of (2) $TBCM_3PP$ and (3) TCM_3IPP compared to (1) TCM_4PP is due to the heavy atom effect. The heavy halogen nuclei induce spin orbital coupling and promote intersystem crossing into the triplet state.[4] Thereby, the heavy atoms quench the excited singlet state.

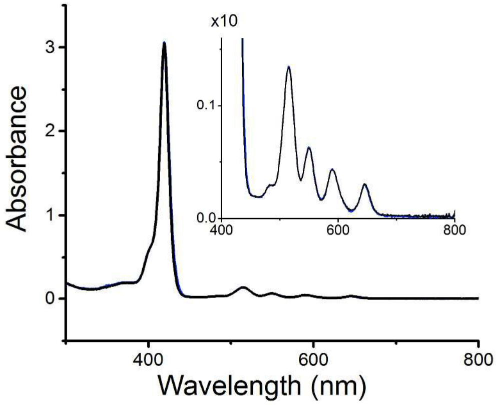

Fig. 2. Superimposed absorption spectra of aerated, 6 x 10^{-6} M solutions of: (1) TCM_4PP (–), (2) $TBCM_3PP$ (–) and (3) TCM_3IPP (–).

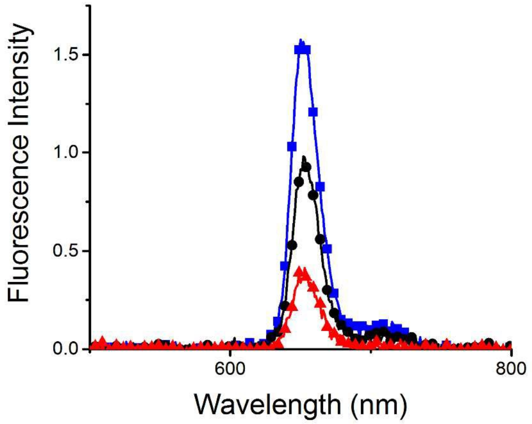

Fig. 3. The emission spectra for the aerated ~ 2 x10^{-5} M solutions of (1) TCM$_4$PP (■),(2) TBCM$_3$PP (•) and (3) TCM$_3$IPP (Δ).

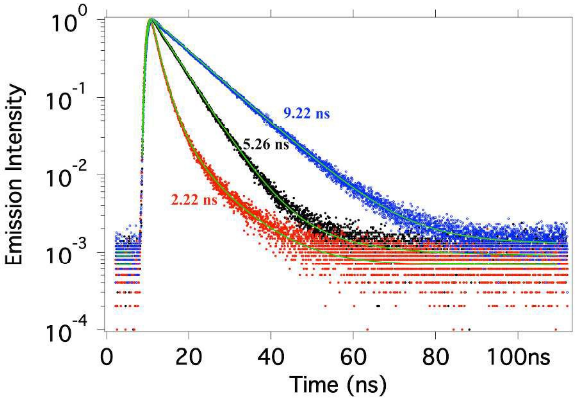

Fig. 4 The normalized decay profiles for ~2.0 x 10^{-5} M aerated solutions of (1) TCM$_4$PP (■) (2) TBCM$_3$PP (•) and (3) TCM$_3$IPP (Δ) with corresponding lifetimes.

Porphyrin	$\boldsymbol{\tau_F}$, ns	$\boldsymbol{\phi_F}$	$\boldsymbol{k_F = \frac{\phi_F}{\tau_F}}$, s^{-1}	$\boldsymbol{\phi_T}$	$\boldsymbol{k_{isc} = \frac{\phi_T}{\tau_F}}$ s^{-1}
TCM$_4$PP	9.22	0.09	9.76 x 10^6	0.35 ± .10	3.80x10^7
TBCM$_3$PP	5.26	0.04	7.60 x 10^6	0.75 ± .10	1.43x10^8
TCM$_3$IPP	2.22	0.02	9.01 x 10^6	0.88 ± .10	3.96x10^8

Table 1. Photophysical Parameters for TCM$_4$PP, TBCM$_3$PP and TCM$_3$IPP

Triplet State Quantum Yields

Bachilo and Weisman have shown that delayed fluorescence arising due to triplet-triplet recombination can be used to accurately calculate triplet quantum yields. However, the delayed fluorescence signal is several orders of magnitude weaker than singlet fluorescence, and may last for hundreds of microseconds. A single short laser pulse (a few hundred femtoseconds long) typically employed to measure fast fluorescence dynamics is insufficient to build up a significant triplet population, in order to observe weak emission by triplet-triplet annihilation. One way to overcome this obstacle is to use excitation pulses of longer duration as employed by Bachilo and Weisman in their study. However, that would make the recording of fluorescence unfeasible. Another way is to use a burst of high repetition rate pulses to build up the triplet state population. The co-authors in this study have previously demonstrated a gated time-resolved fluorescence technique that involves exciting a sample with a controllable number of 80 MHz laser pulses.[15] Without any change in the optical setup, a simple variation in the length of the electronic gate signal allows us to vary the number of excitation pulses from one to the number desired.

In this study, we use the above mentioned multi-pulse time resolved fluorescence technique (see experimental methods for more detail) to excite each sample with a pulse train consisting of 100 pulses with an inter-pulse separation of 12.5 ns. Figure 5 shows the multi-pulse prompt and delayed fluorescence decays for various samples. Clearly, the emission decay consists of a fast singlet fluorescence peak in the early period, and a weak but very long decay component building up on account of triplet-triplet recombination.

The triplet quantum yield for porphyrins were calculated as described previously and shown in equation 2:

$$\phi_T = \frac{5}{1+Qk_A} \tag{2}$$

where Q is calculated as the area under the prompt divided by the intensity of the delayed fluorescence at time zero.[14] The prompt fluorescence represents the fast component of fluorescence emission, when the electron recombines with a hole after occupying the singlet state only. The prominence of the prompt fluorescence with respect to delayed fluorescence is clearly visualized when displayed on the full linear axis, where the delayed fluorescence makes a negligible contribution. The second order rate constant for triplet-triplet annihilation, k_A, was found by fitting the intensity of the delayed fluorescence to equation 3.[14]

$$I_{DF} = \alpha \frac{k_{TT}^{Enc}}{9} \phi_F \left(\frac{\left[{}^3S^* \right]_0}{1+k_A t \left[{}^3S^* \right]_0} \right)^2 \tag{3}$$

The variable α represents instrument sensitivity, k_{TT}^{Enc} is the triplet-triplet encounter rate constant, and $[\,{}^3S^*]_0$ stands for the concentration of triplets at t equal to zero, where t is time. The multi-pulsed triplet-triplet annihilation technique was performed using 5,10,15,20-tetraphenylporphyrin as the control and a triplet quantum yield matching the literature value was obtained.[14] The prompt and delayed fluorescence decay profiles for the three derivatives are shown in Figure 5. Their corresponding averaged lifetimes are displayed as well. A comparison of the delayed fluorescence reveals that TCM$_3$IPP has the highest intensity of delayed fluorescence, which decays at a faster rate than the other two derivatives. TBCM$_3$PP has the second highest intensity of triplet-triplet annihilation followed by TCM$_4$PP. The triplet quantum yields and their corresponding rate of intersystem crossing are listed in Table 1.

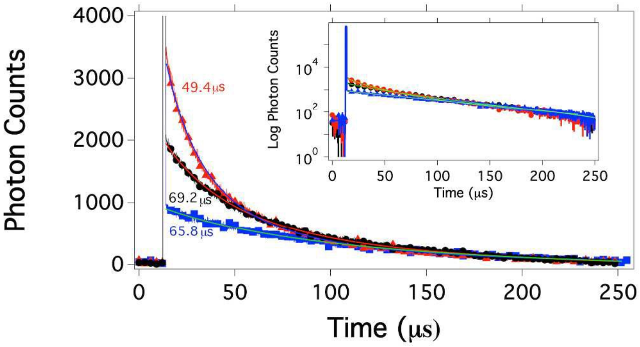

Fig. 5 Delayed fluorescence of 1) TCM_4PP (■), 2) $TBCM_3PP$ (•) and 3) TCM_3IPP (Δ) with excitation pulse at 12.5 μs and average lifetimes. The inset shows the normalized overlaid prompt fluorescence on a logarithmic scale for 1) TCM_4PP (■), 2) $TBCM_3PP$ (•) and 3) TCM_3IPP (Δ).

The triplet quantum yield for TCM_4PP is 0.35 which is 50% lower than the triplet quantum yield for tetraphenylporphyrin ($\phi_T = \sim 0.70$).[7, 14] This indicates that the carbomethoxy groups destabilize the singlet to triplet transition. Nevertheless, substituting an iodine for one of the carbomethoxy substituents on TCM_4PP increases the efficiency of triplet formation by 151% to 0.88. Such a large increase is impressive when considering the non-planarity and distance of the iodophenyl substituent from the conjugated porphyrin core of π electrons. The calculated triplet quantum yield for $TBCM_3PP$ increased 114% to 0.75. The rates of intersystem crossing were calculated as 3.80×10^7 s^{-1}, 1.43×10^8 s^{-1}, and 3.96×10^8 s^{-1} for TCM_4PP, $TBCM_3PP$ and TCM_3IPP respectively. The increasing efficiency of triplet formation in the presence of a heavy halogen is a direct consequence of the interaction between the magnetic field produced by the heavy atom and the magnetic moment of the molecule's valence electron, which has been excited into the LUMO level by the electric field of the exciting light.[10] Iodine, the heaviest atom, has the most pronounced increase in the efficiency of triplet formation because it is larger and therefore has the strongest spin orbit coupling.

Singlet Oxygen Quantum Yields

Chemical Quenching with DPBF

Singlet oxygen is generated as a result of energy transfer from a triplet state porphyrin to molecular oxygen and therefore is often a good indicator of triplet formation. The quantum yields of singlet oxygen were determined using chemical quenching of DPBF and the comparative method with singlet oxygen emission. The efficiency of DPBF oxidation was calculated according to equation 4.[20, 22-24]

$$\phi_{\mathrm{DPBF}} = \frac{\frac{\partial[\mathrm{DPBF}]}{\partial \mathrm{t}}}{I_{\mathrm{a}}} = \phi_{\Delta}\left(\frac{k_{\mathrm{r}}[\mathrm{DPBF}]}{k_{\mathrm{r}}[\mathrm{DPBF}] + k_{\mathrm{d}}}\right) \qquad (4)$$

In equation 4, t is the time interval, I_a represents the number of photons absorbed per unit time, k_r is the rate constant for the reaction between singlet oxygen and DPBF and k_d is the rate constant for the decay of singlet oxygen.[20, 22-24] Conventionally ϕ_Δ, the singlet oxygen quantum yield, is obtained from Stern-Volmer plots of the data as shown in equation 5.[20, 22, 23, 25]

$$\frac{1}{\phi_{\mathrm{DPBF}}} = \frac{1}{\phi_{\Delta}} + \frac{k_{\mathrm{d}}}{k_{\mathrm{r}}\phi_{\Delta}[\mathrm{DPBF}]} \qquad (5)$$

However, low coefficients of determination were obtained due to small variations in the change in DPBF concentration, even though the time intervals were constant. Therefore another approach, reported by Figueiredo et al., was applied in which equation 1 was integrated to yield equation 6.[23, 26]

$$\left[\Delta[\mathrm{DPBF}] + \frac{k_{\mathrm{d}}}{k_{\mathrm{r}}}\ln\frac{[\mathrm{DPBF}]_{\mathrm{t}}}{[\mathrm{DPBF}]_{\mathrm{o}}}\right] = -I_{\mathrm{a}}\phi_{\Delta}t \qquad (6)$$

The reported value for $k_d k_r^{-1}$ in DMF is 2×10^{-5}.[27] I_a in equation 6 represents the moles of photons absorbed per unit time and volume, and is calculated using equation 7.

$$I_{\mathrm{a}} = (1-10^{-Abs_{\lambda\mathrm{ex}}})\left(\frac{A \cdot N_{\mathrm{p}}}{N_{\mathrm{A}}\ V}\right) \qquad (7)$$

$Abs_{\lambda ex}$ is the absorbance of the photosensitizer at the excitation wavelength, A represents the area of irradiation, N_A is Avogadro's number and V is the reaction volume. N_p is the number of photons per unit area per second and is calculated according to equation 8,

$$N_{\mathrm{p}} = \frac{P\lambda_{\mathrm{ex}}}{hc} \qquad (8)$$

where P is power, λ_{ex} is the wavelength of light exposure, h is Planks constant and c is the speed of light. The singlet oxygen quantum yield was determined by dividing the slope generated from the graph of the left side of equation 6 with respect to time, by I_a. The extinction coefficient used for DPBF in DMF at 408 nm was 20,744 L mol^{-1} cm^{-1}. Quantum yields for singlet oxygen generation were acquired by measuring the change in DPBF concentration as a function of illumination time with 552 nm light. Fig. 6 shows the depletion of DPBF with time of light exposure for (1) TCM_4PP, (2) $TBCM_3PP$ and (3) TCM_3IPP. This data was applied to equation 6 and the plot generated is shown in Fig. 7. As indicated in Table 2, the singlet oxygen quantum yields were calculated as 0.54 ± 0.07, .74 ± 0.02 and 0.91 ± 0.06 for (1) TCM_4PP, (2) $TBCM_3PP$, and (3) TCM_3IPP. The upward trend in singlet oxygen generation with increasing mass of heavy atom substituent is a direct result of the heavy atom effect. The spin orbit coupling produced by iodine or bromine facilitates intersystem crossing into the triplet state, which enables energy transfer to molecular oxygen.[1, 5, 22, 23, 28, 29] Energy transfer from the porphyrin in the triplet state to molecular oxygen generates singlet oxygen, which then degrades DPBF.[30]

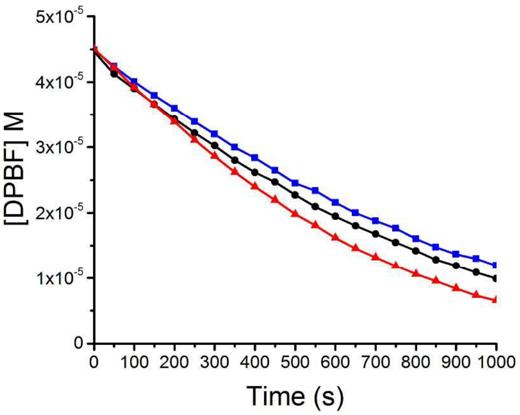

Fig. 6 Normalized DPBF concentration as a function of time during singlet oxygen quenching with (1) TCM_4PP (■), (2) $TBCM_3PP$ (•) and (3) TCM_3IPP (Δ).

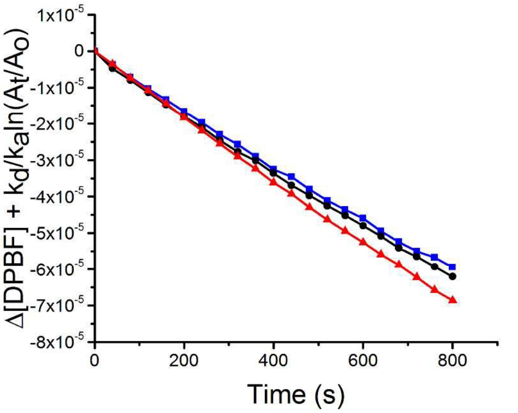

Fig.7 The data for singlet oxygen quenching applied to equation 6. Equation 6 is the sum of the change in DPBF concentration and the product of k_d/k_a with the natural logarithm of the quotient of DPBF absorption at final and initial time periods. Singlet oxygen quantum yield were calculated by dividing the slope of the line by I_a. I_a was calculated using equation 7. The singlet oxygen quantum yields for 1) TCM4PP, 2) TBCM3PP and 3) TCM3IPP are 0.54 ± 0.07, 0.74 ± 0.02 and 0.91 ± .06.

Comparative method with Singlet Oxygen Emission

Low coefficients of determination and overlap of the porphyrin absorption peak with the absorption of DPBF (subtractions were performed) motivated us to determined the singlet oxygen quantum yield using the comparative method of singlet oxygen emission. Equation 8 was used to calculate the singlet oxygen quantum yield. TPP was used as the standard with a reported quantum yield of 0.7.[31]

$$\phi_\Delta = \phi_\Delta^{Std}\,\frac{I}{I_{Std}}\,\frac{1-10^{-A_{Std}}}{1-10^{-A}} \qquad (8)$$

The singlet oxygen emission profiles for all three compounds are shown in Fig. 8 and the quantum yields were measured as 0.47 for (1) TCM_4PP, 0.76 for (2) $TBCM_3PP$ and 0.89 for (3) TCM_3IPP, as shown in Table 2.

Porphyrin	ϕ_Δ^a	ϕ_Δ^b
TCM_4PP	0.54 ± 0.07	0.47 ± .11
$TBCM_3PP$	0.74 ± 0.02	0.76 ± .03
TCM_3IPP	0.91 ± .06	0.89 ± .02

Table 2. Singlet oxygen quantum yields determined using a) chemical quenching of DPBF and b) the comparative method with singlet oxygen emission.

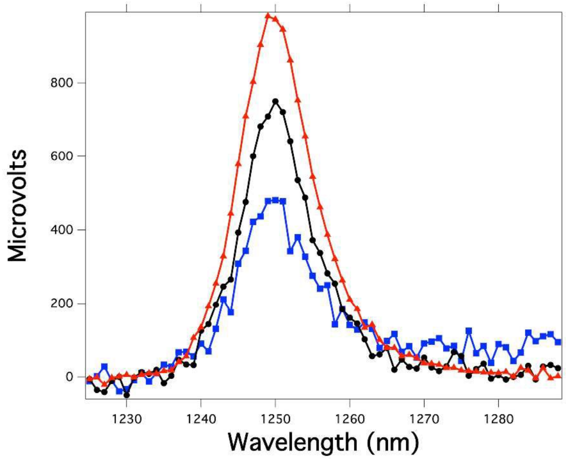

Figure 8. Singlet Oxygen Emission of 2 x10^{-5} M solutions of (1) TCM_4PP (■), (2) $TBCM_3PP$ (•) and (3) TCM_3IPP (Δ) in toluene.

The singlet oxygen quantum yields obtained for (1) TCM_4PP using both methods are approximate to the singlet oxygen quantum yield of 0.49 reported in chloroform.[12] These experiments indicates that only one iodine atom on the meso phenyl ring of the porphyrin molecule is necessary to achieve a 69% - 89% increase in the singlet oxygen quantum yield. A smaller, yet significant 37% - 61% increase in the singlet oxygen quantum yield is observed with a single bromine atom. The differences in the singlet oxygen quantum yields acquired for each sample, using the two different methods, is no greater than ten percent. This indicates that the two different methods are comparable and that the values obtained are reliable.

Experimental

Materials

The mixed-substituent porphyrin derivatives were synthesized and purified according to previous methods.[32] Triethylamine, leutidine, dichloromethane, 1,3-diphenylisobenzofuran, pyrrole and N,N-dimethylformamide were obtained from Sigma-Aldrich. All chemicals were used as supplied except pyrrole, which was distilled before use.

Absorption, Emission and Lifetime Measurements

Absorption, fluorescence emission, and fluorescence lifetime measurements were taken on aerated and degassed solutions of approximately 2 x 10^{-5} M in DCM. Triethylamine or leutidine (~10 µL/4 mL) was added to prevent protonation and outgassing was accomplished using the pump-freeze-thaw method. A Varian Cary 300 spectrometer was used to detect absorption. Steady state fluorescence emission and excitation were measured on a Shimadzu RF5301 PC fluorometer or on a Jobin Yvon Fluorolog 3. Time correlated single photon counting was obtained on the Fluorolog equipped with a 341 nm photodiode laser. The lifetimes of the corresponding derivatives were obtained by fitting the data using IGOR Pro software.

Fluorescence Quantum Yields

The fluorescence quantum yields were determined in DCM using 552 nm as the excitation wavelength. Absorption at the excitation wavelength was measured on the Cary 300 and emission was measured on a Shimadzu RF5301 PC fluorometer. The excitation and emission slit widths were 1.5 nm and the integrated area of each emission peak was measured using "Fluorescence" software.

Triplet Quantum Yields

Triplet−Triplet annihilation fluorescence was recorded using a femtosecond Ti:saphire laser (Spectra Physics MaiTai), operating at 80 MHz repetition rate and 820 nm. The laser output was fed to an optical parametric oscillator (OPO) (Spectra Physics Inspire). The frequency-doubled output (410 nm) from the OPO was then directed through two electro-optic modulators (Conoptics 350-105 KD*P Series) driven by a high voltage push–pull power amplifier. A delay generator (SRS DG535), externally triggered by a synchronous counter operating at 4 kHz, was used to produce an electronic gate of variable length, which determined the length of the optical gate opened by the pulse-picker system. An electronic gate of suitable length was chosen to excite the sample with 100 pulses. The excitation light was focused on a degassed sample solution inside a 10 mm sealed quartz cuvette. Fluorescence dynamics were measured by time correlated single photon counting, using a multichannel photon counting board (Becker & Hickl DPC 230) with a double monochromator (Spectral Products CM112) and a hybrid PMT detector (Becker&Hickl HPM-100-40). The delayed fluorescence data was fit using IGOR Pro software with the second order rate constant for triplet-triplet annihilation constrained between 13,000 and 24,000 s^{-1}.

Singlet Oxygen Quantum Yields

The quantum yield for singlet oxygen was determined by chemical quenching with DPBF in DMF using 552 nm monochromatic light from a Newport monochromator and xenon lamp similar to methods already reported.[20, 22, 23] To summarize, a reaction mixture (4 mL) of DPBF (~5 x 10^{-5} M) and porphyrin (5–10 x10^{-6} M) was prepared and promptly dispensed in a (1 cm x 1 cm) quartz cuvette. The absorbance of the reaction was monitored at 552 nm to determine the absorption of the photosensitizer at the excitation wavelength and at 408 nm to monitor DPBF depletion. The reaction was mixed as it was illuminated. Light exposure was maintained for timed intervals (30 - 100 s) which produced a ~5% change in DPBF concentration. The timed light exposure was controlled with a shutter and the intensity was measured using a Newport silicon detector connected to a CEN-TECH digital multi-meter. The average measured light intensity was ~ 4.9 W m^{-2}. A reference spectrum of the porphyrin in DMF was taken before each experiment and subtracted from the final data. The experiments were performed at least three times for each sensitizer and at least fourteen timed intervals were measured. The comparative method of singlet oxygen emission was performed on aerated 2x10^{-5} M solutions. The emission was filtered with an 850 nm long pass filter and the resulting spectrum is an average of 10 scans with an integration time of 2 seconds each. The samples were excited with 514 nm light with an excitation slit width of 14.7 nm and an emission slit width of 10 nm. The spectra were corrected for dark counts and for excitation light fluctuations.

Conclusion

The decrease in emission, lifetime and fluorescent quantum yields, and increase in the triplet and singlet oxygen quantum yields is a consequence of the "heavy atom effect". The prudent use of just one heavy halogen substituent and its considerable effect on triplet formation and singlet oxygen generation is noteworthy and allows for further functionalization of the molecule. We envision that the remaining three carbomethoxy groups can be used as molecular modification points for nanoparticle formation or for possible targeting ligands.[33] The high triplet and singlet oxygen quantum yields of the heavy atom derivatives implies that they are suitable candidates for photodynamic therapy and for solar cells designed to extract electrons from the triplet state. The triplet state quantum yields were measured by applying a multi-pulsed excitation in order to build a significant triplet population for analysis with Weisman's triplet-triplet annihilation method.[14, 15] The singlet oxygen quantum yields calculated using chemical quenching of DPBF and singlet oxygen emission match the reported value for TCM_4PP within standard deviation, and the singlet oxygen quantum yields for $TBCM_3PP$ and TCM_3IPP are within standard deviations of each other.[14, 15]

Acknowledgements

This research was funded by the Department of Chemistry at the University of North Carolina at Charlotte, Nanoscale Science Ph.D. program, and through a UNC Charlotte Faculty Research Grant (#111726). MGW also acknowledges NSF – REU support for SP supported by the NSF REU site program in partnership with the ASSURE program of the DoD (CHE 1156867).

Notes and references

Department of Chemistry, Burson 200, 9201 University City Blvd., Charlotte, NC 28223-0001
*Correspondences to Michael.Walter@uncc.edu

† Abbreviations: PDT, photodynamic therapy; FDA, Food and Drug Administration; DCM, dichloromethane; DMF, N,N-dimethylformamide; DPBF, 1,3-diphenylisobenzofuran; TCM_4PP, 5,10,15,20-tetrakis(4-carbomethoxyphenyl)porphyrin; $TBCM_3PP$, 5,10,15-tris(4-carbomethoxyphenyl)-20-(p-bromophenyl)porphyrin; TCM_3IPP, 5,10,15-tris-(4-carbomethoxyphenyl)-20-(p-iodophenyl)porphyrin;

1. P. Agostinis, K. Berg, K. Cengel, T. Foster, A. Girotti, S. Gollnick, S. Hahn, M. Hamblin, A. Juzeniene, D. Kessel, M. Korbelik, J. Moan, P. Mroz, D. Nowis, J. Piette, B. Wilson and J. Golab, Photodynamic Therapy of Cancer: An Update, *CA Cancer J Clin*, 2011, **61**, 250-281`.
2. D. D. Ethan Sternberg, Porphyrin-Based Photosensitizers for Use in Photodynamic Therapy, *Tetrahedron*, 1998, **54**, 4151-4202.
3. C.-M. Yang, C.-H. Wu, H.-H. Liao, K. Y. Lai, H.-P. Cheng and S.-F. Horng, Enhanced Photovoltaic Response of Organic Solar Cells by Singlet To Triplet Exciton Conversion, *Applied Physics Letters*, 2007, **90**, 133509.
4. J. Zhao, W. Wu, S. Jifu and S. Guo, Triplet Photosensitizers: From Molecular Design to Applications, *Chem. Soc. Rev.*, 2013, **42**, 5323-5351.
5. A. Ormond and H. Freeman, Dye Sensitizers for Photodynamic Therapy, *Materials*, 2013, **6**, 817-840.
6. R. Bonnett, H. Anthony and A. Kozyrev, Photophysics of Halogenated Porphyrins, *J. Chem. Soc. Faraday Trans.*, 1992, **88**, 763-769.
7. E. Azenha, A. C. Serra, M. Pineiro, M. M. Pereira, J. Seixas de Melo, L. G. Arnaut, S. J. Formosinho and A. M. d. A. R. Gonsalves, Heavy atom effects on the metalloporphyrins and polyhalogentated porphyrins, *Chemical Physics*, 2002, **280**, 177-190.
8. M. Laranjo, A. C. Serra, M. Abrantes, M. Pineiro, A. C. Goncalves, J. Casalta-Lopes, L. Carvalho, A. B. Sarmento-Ribeiro, A. Rocha-Gonsalves and F. Botelho, 2-Bromo-5-hydroxyphenylporphyrins for Photodyanmic Therapy: Photosensitization Efficiency, Subcellular Localization and In Vivo Studies, *Photodiagnosis and Photodyanmic Therapy*, 2013, **10**, 51-61.
9. A. C. Serra, M. Pineiro, A. M. d. A. R. Gonsalves, M. Abrantes, M. Laranjo, A. C. Santos and M. F. Botelho, Halogen atom effect on photophysical and photodynamic characteristics of derivatives of 5,10,15,20-tetrakis93-hydroxyphenyl)porphyrin, *Journal of Photochemistry and Photobiology B: Biology*, 2008
, **92**, 59-65.
10. P. W. Atkins, *Quanta A Handbook of Concepts, 2nd ed.*, Oxford University Press, Oxford, New York, Tokyo, 2nd edn., 1991.
11. F. Nifiatis, J. C. Athas, K. D. D. Gunaratne, Y. Gurung, K. M. Monette and P. J. Shivokevich, Substituent Effects of Porphyrin on Singlet Oxygen Generation Quantum Yields, *The Open Spectroscopy Journal*, 2011, **5**, 1-12.
12. V. F. Ferreira, D. Ferreira, A. Oliveira, R. Boscencu, R. Socoteanu, M. Ilie, C. Constantin and M. Neagu, Synthesis, photophysical and cytotoxicity evaluation of A3B type mesoporphyrinic compounds, *Dyes and Pigments*, 2012, **95**, 296-303.
13. D. Quimby and L. Frederick, Luminescence Studies of Several Tetraarylporphyrins and thier Zinc Derivatives, *Journal of American Chemical Society*, 1975, **97**, 5111-5117.
14. S. M. Bachilo and R. B. Weisman, Determination of Triplet Quantum Yields from Triplet-Triplet Annihilation Fluorescence, *The Journal of Physical Chemistry A*, 2000, **104**, 7711-7714.
15. G. Singh, M. Guericke, Q. Song and M. Jones, A Multipulse Time-Resolved Fluorescence Method for Probing Second-Order Recombination Dynamics in Colloidal Quantum Dots, *The Journal of Physical Chemistry C*, 2014, **118**, 14692-14702.
16. L. Milgrom, *The Colours of Life*, Oxford University Press, New York, 1997.
17. M. Allen, Measurement of Fluorescence Quantum Yields, in *PDF*, ed. T. F. Scientific, Thermo Fisher Scientific, http://www.researchgate.net, 2010, p. 4.---
18. J. R. Lakowicz, *Principles of Fluorescence Spectroscopy Third ed.*, Springer Science and Business Media, LLC, 233 Springer St, New York, NY, 2006.
19. A. T. Rhys Williams and S. A. Winfield, Relative Fluorescence Quantum Yields Using a Computer-Controlled Luminescence Spectrometer, *Analyst*, 1983, **108**, 1067-1071.
20. M. P. Donzello, E. Viola, M. Giustini, C. Ercolani and F. Monacelli, Tetrakis(thiadiazole)porphyrazines. 8. Singlet Oxygen Production, Fluoresence Response and Liposomal Incorporation of Tetrakis(thiadiazole)porphyrazine macrocycles [TTDPzM] (M=MgII(H2O), ZnII, Al III, Cl, GaIIICl, CdII,CuII, 2H1), *Dalton Transactions*, 2012, **41**, 6112- 6120.
21. C. Barker, X. Zeng, S. Bettington, A. Batsanov, M. Bryce and A. Beeby, Porphyrins Phthalocyanines and Porphyrazines Derivatives with Multifluorenyl Substituents as Efficient Deep-Red Emitters, *Chemistry A European Journal*, 2007, **13**, 6710-6717.
22. W. Spiller, H. Kliesch, D. Wohrle, S. Hackbarth, B. Roder and G. Schnurpfeil, Singlet Oxygen Quantum Yields of Different Photo-sensitizers in Polar Solvents and Micellar Solutions, *Journal of Porphyrins and Phthalocyanines*, 1998, **2**, 145-158.
23. T. L. C. Figueiredo, Johnstone R. A. W., S. S. A. M. P., D. Burget and P. Jacques, Determination of Fluorescence Yields, Singlet Lifetimes and Singlet Oxygen Yields of Water-Insoluble Porphyrins and Metalloporphyrins in Organic Solvents and in Aqueous Media, *Photochemistry and Photobiology*, 1999, **69**, 517-528.
24. F. Wilkinson, P. W. Helman and A. B. Ross, Quantum Yields for the Photosensitized Formation of the Lowest Electronically Excited Singlet State of Molecular Oxygen in Solution, *Journal of Physical and Chemical Reference Data*, 1993, **22**, 113-262.

25. P. B. Merkel and W. G. Herkstroeter, The Fate Of Oxygen In The Quenching Of Excited Singlet States, *Chemical Physics Letters*, 1978, **53**, 350-354.
26. R. Venkatesan, N. Periasamy and T. S. Srivastava, Singlet Molecular Oxygen Quantum Yield Measurements of Some Porphyrins and Metalloporphyrins, *Proc. Indian Acad. Sci. (Chem. Sci.)*, 1992, **104**, 713-722.
27. F. Wilkinson, P. W. Helman and A. B. Ross, Rate Constants for the Decay and Reactions of the Lowest Electronically Excited Singlet State of Molecular Oxygen in Solution. An Expanded and Revised Compilation, *Journal of Physical and Chemical Reference Data*, 1995, **24**, 663-911.
28. K. Plaetzer, B. Krammer, J. Berlanda, F. Berr and T. Kiesslich, Photophysics and photochemistry of photodynamic therapy: fundamental aspects, *Lasers Med Sci*, 2009, **24**, 259-268.
29. E. Nyman and P. Hynninen, Research Advances in the use of tetrapyrrolic photosensitizers for photodynamic therapy, *Journal of Photochemistry and Photobiology B: Biology*, 2004, **73**, 1-28.
30. X.-F. Zhang and X. Li, The photostability and fluorescence properties of diphenylisobenzofuran, *Journal of Luminescence*, 2011, **131**, 2263-2266.
31. W. Shao, H. Wang, S. He, Shi, Lei, K. Peng, Y. Lin, L. Zhang, L. Ji and H. Liu, Photophysical Properties and Singlet Oxygen Generation of Three Sets of Halogenated Corroles, *The Journal of Physical Chemistry B*, 2012, **116**, 14228-14234.
32. A. L. Ortiz, G. C. Collier, D. M. Marin, R. J. Ivins, N. G. Grubich and M. G. Walter, The Effects of Heavy Atoms on the Exciton Diffusion Properties in Photoactive Thin Films of Tetrakis(4-carbomethoxyphenylporphyrins, *J. Mater. Chem. C*, 2014, in prog.
33. J. L. Vivero-Escoto and D. L. Vega, Stimuli-responsive protoporphyrin IX silica-based nanoparticles for photodynamic therapy in vitro, *RSC Adv.*, 2014, **4**, 14400-14407.